Bandwidth Scaling and Diversity Gain for Ranging and Positioning in Dense Multipath Channels

Klaus Witrisal, *Member, IEEE,* Erik Leitinger, *Student Member, IEEE,* Stefan Hinteregger, *Student Member, IEEE,* and Paul Meissner, *Member, IEEE*

***Abstract*—The Cramér-Rao lower bound (CRLB) on the ranging error variance is revisited to quantify the influence of dense multipath in indoor environments. Our analytical results yield novel insight on the scaling of the ranging and positioning accuracy as a function of bandwidth and number of diversity branches. It also yields insight in the detectability of the useful line-of-sight signal component. It is found that the Fisher information scales faster than quadratically in bandwidth but only linearly in the number of independent diversity branches. We investigate the entire bandwidth-range from the flat-fading narrowband case up to ultra-wideband.**

***Index Terms*—Cramér-Rao bound, dense multipath channels, ranging, positioning, indoor environments, diversity, MIMO.**

I. Introduction

ACCURATE indoor positioning remains a profound challenge. Lacking availability and insufficient accuracy of global satellite-based positioning systems, limited bandwidth of current wireless standards, and a heterogeneity of application scenarios are among the main reasons hindering the adoption of indoor positioning systems.

The study of performance bounds allows for fundamental insights on the system requirements and design principles. For example in [1], [2], the Cramér Rao lower bound (CRLB) has been used to investigated the performance limits of radiopositioning and radar systems. These results yield insight in the influence of the anchor geometry and signal parameters such as bandwidth (BW) and signal-to-noise ratio (SNR).

For indoor positioning, ultra-wideband (UWB) radio signals have been considered most promising, because individual multipath components (MPC) can potentially be separated from each other at the resulting fine time resolution. For example in [3], the CRLB and the Ziv-Zakai Bound (ZZB) have been discussed for the stochastic IEEE 802.15.4a UWB channel model. The ZZB yields insight in the detectability of the information-bearing line-of-sight (LOS) signal component. The additional information comprised in geometrically modeled deterministic components has been quantified in [4], modeling the channel as a combination of specular reflections and so-called dense or diffuse multipath (DM) [5].

The reduced BW of non-UWB radio systems leads to massive path-overlap preventing the separation of different geometric propagation paths. For a flat fading channel, the DM completely interferes with the LOS component, while for the UWB case the LOS component is separated from the DM. BWs in-between these "extreme" cases lead to substantial distortion and fading of the received LOS signal simultaneously. In [1] a path-overlap coefficient is introduced to quantify multipath interference in the first contiguous cluster of arriving signal components. The impact of multipath on energy-detector-based ranging has been analyzed in [6].

In this letter, we revisit the performance limit of radio-based ranging and positioning *in presence of dense multipath*. We introduce a Gaussian stochastic model for the diffuse multipath, formulate and analyze the CRLB on the ranging and positioning performance, and show how diversity combining of quasi-co-located but independent ranging measurements scales the ranging error bound (REB) and the position error bound (PEB). Our results are useful for accounting for the impact of DM in indoor channels, e.g., for the optimization of network localization techniques [7]–[9] or for the design and analysis of array-based positioning [10], [11].

II. Signal Model

We consider L measurements obtained from signal transmissions among an agent at unknown position $\mathbf{p}$ and anchors at known positions $\mathbf{a}_\ell$, $\ell = 1, \ldots, L$. A signal $s(t)$ is transmitted; the corresponding baseband equivalent received signal is modeled as [4]

$$r_\ell(t) = \alpha_\ell s(t - \tau_\ell) + (s * \nu_\ell)(t) + w(t) \tag{1}$$

where the first term is the LOS component with complex amplitude α_ℓ and delay τ_ℓ. The delay is deterministically related to the agent and anchor positions, expressed by e.g. $\tau_\ell = \frac{1}{c}\|\mathbf{p} - \mathbf{a}_\ell\|$ for active positioning with an anchor at position $\mathbf{a}_\ell$. Constant c is the speed of light. We assume the energy of $s(t)$ to be normalized to one, hence $|\alpha_\ell|^2$ is the energy of the LOS component of measurement ℓ.

The second term denotes the convolution of the transmitted signal $s(t)$ with a random process $\nu_\ell(t)$ that accounts for dense multipath (DM). We assume uncorrelated scattering along the delay axis t, hence the auto-correlation function of $\nu_\ell(t)$ is

$$K_\nu^{(\ell)}(t, u) = \mathbb{E}_\nu \left\{ \nu_\ell(t) \nu_\ell^*(u) \right\} = S_\nu^{(\ell)}(t - \tau_\ell)\delta(t - u) \tag{2}$$

where $S_\nu^{(\ell)}(t)$ is the power delay profile (PDP) of the DM at the agent position $\mathbf{p}$ as a function of the excess delay time. The DM process is assumed to be a zero-mean Gaussian process that is quasi-stationary in the spatial domain, which means that $S_\nu^{(\ell)}(t)$ does not change in the vicinity of position $\mathbf{p}$.

Finally, $w(t)$ denotes additive white Gaussian noise (AWGN) with double-sided power spectral density $N_0/2$.

III. Ranging Error Bound

To investigate the BW scaling of the ranging error variance in presence of DM, we derive the REB, defined as the square

Manuscript received January 29, 2016; revised April 18, 2016; accepted May 10, 2016.

The authors are with Graz University of Technology, Austria; email: witrisal@tugraz.at. This work was supported by the Austrian Research Promotion Agency (FFG) within the project REFlex (project number: 845630).

root of the inverse of the equivalent Fisher information (EFI) $\mathcal{R}(\tau) = \sqrt{\mathcal{I}_\tau^{-1}}$, the square root of the CRLB $\mathrm{var}\{\hat{\tau}\} \geq \mathcal{I}_\tau^{-1}$ for the delay-estimation problem. For simplicity, we drop the measurement index ℓ. The EFI can be computed from the likelihood function $f(\mathbf{r}|\boldsymbol{\psi})$ for the received signal $\mathbf{r}$ conditioned on parameter vector $\boldsymbol{\psi} = [\tau, \Re\alpha, \Im\alpha]^{\mathrm{T}}$ which comprises delay τ and real and imaginary parts of amplitude α. This likelihood function is defined, under the Gaussian assumption and for a sampled received signal vector $\mathbf{r} = [r(0), r(T_\mathrm{s}), \ldots, r((N-1)T_\mathrm{s})]^{\mathrm{T}} \in \mathbb{C}^N$, by

$$f(\mathbf{r}|\boldsymbol{\psi}) \propto \exp\left\{-(\mathbf{r} - \mathbf{s}_\tau\alpha)^{\mathrm{H}}\mathbf{C}_\mathrm{n}^{-1}(\mathbf{r} - \mathbf{s}_\tau\alpha)\right\} \tag{3}$$

where $\mathbf{s}_\tau$ is a delayed version $\mathbf{s}_\tau = [s(-\tau), s(T_\mathrm{s} - \tau), \ldots, s((N-1)T_\mathrm{s} - \tau)]^{\mathrm{T}}$ of the sampled transmit signal and $\mathbf{C}_\mathrm{n} = \sigma_\mathrm{n}^2\mathbf{I}_N + \mathbf{C}_\mathrm{c} \in \mathbb{R}^{N\times N}$ denotes the covariance matrix of the noise processes. The inverse of the covariance matrix represents a whitening operation to account for the (nonstationary, colored) noise process [12]. To gain insight in this operation, we write $\mathbf{C}_\mathrm{n} = \sum_{i=0}^{N-1}\mathbf{u}_i\mathbf{u}_i^{\mathrm{H}}(\lambda_i + \sigma_\mathrm{n}^2)$ where $\mathbf{u}_i$ and $\lambda_i \in \mathbb{R}$ are the i-th eigenvector and eigenvalue of $\mathbf{C}_\mathrm{c}$ (see the appendix). Note that λ_i quantifies the DM power in direction of $\mathbf{u}_i$ while $\sigma_\mathrm{n}^2 = N_0/T_\mathrm{s}$ is the variance of the AWGN samples. Using this expansion, we introduce the Fourier-weighted inner product (in the Hilbert space $\mathcal{H}$)

$$\langle \mathbf{x}, \mathbf{y}\rangle_\mathcal{H} = \sigma_\mathrm{n}^2\mathbf{y}^{\mathrm{H}}\mathbf{C}_\mathrm{n}^{-1}\mathbf{x} \tag{4}$$

$$= \sum_{i=0}^{N-1}\frac{\mathbf{y}^{\mathrm{H}}\mathbf{u}_i\mathbf{u}_i^{\mathrm{H}}\mathbf{x}}{\lambda_i/\sigma_\mathrm{n}^2 + 1} \tag{5}$$

and the induced norm $\|\mathbf{x}\|_\mathcal{H}^2 = \langle \mathbf{x}, \mathbf{x}\rangle_\mathcal{H}$ and obtain—as shown in the appendix—the EFI for the delay parameter τ as

$$\mathcal{I}_\tau = 2\frac{|\alpha|^2}{\sigma_\mathrm{n}^2}\|\dot{\mathbf{s}}_\tau\|_\mathcal{H}^2\sin^2(\varphi) + \mathrm{tr}\left[\mathbf{C}_\mathrm{n}^{-1}\frac{\partial\mathbf{C}_\mathrm{n}}{\partial\tau}\mathbf{C}_\mathrm{n}^{-1}\frac{\partial\mathbf{C}_\mathrm{n}}{\partial\tau}\right] \tag{6}$$

where $\dot{\mathbf{s}}_\tau = \partial\mathbf{s}_\tau/\partial\tau$ is the derivative of $s(t-\tau)$ with respect to τ and φ is the angle between $\dot{\mathbf{s}}_\tau$ and $\mathbf{s}_\tau$ in $\mathcal{H}$.

The first part of (6) is for the delay estimation from the deterministic LOS signal $\alpha\mathbf{s}_\tau$, while the second part quantifies *additional* delay information provided by the DM process. [1] In LOS situations—which are the focus of this paper—the former will by far dominate over the latter. The reason for this is the stochastic nature and the much longer time-extent (unless the bandwidth is very low) of the DM in contrast to the deterministic LOS component. A numeric validation of this proposition is included in Fig. 2 (see "REB w/ PDP estim."). It shows that indeed the impact is negligible in the more-relevant high-bandwidth region. We thus limit the further discussion to the first part of (6), written as $\mathcal{I}_\tau^{(\mathrm{I})}$.

Discussion: It is evident from (5) that the impact of DM is influenced by the interference-to-noise power ratio (INR), because the DM power is expressed by the level of the eigenvalues. In case of negligible DM, we get the well-known AWGN case [12] with

$$\mathcal{I}_\tau^{(\mathrm{AWGN})} = 8\pi^2\beta^2\mathrm{SNR} \tag{7}$$

[1] We assume that other parameters of the DM (e.g. its total power and the shape of the PDP) can be estimated from an ensemble of past measurements.

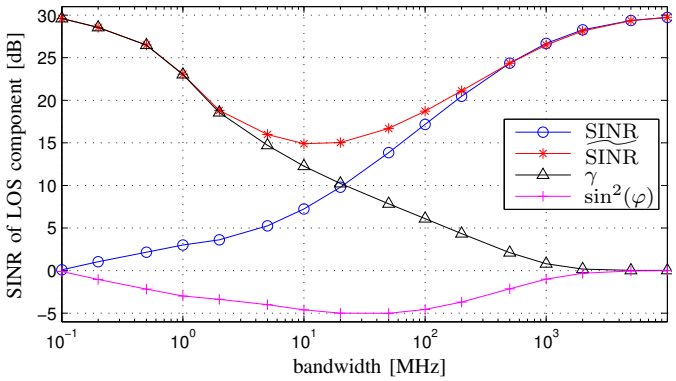

Fig. 1. SINR, $\widetilde{\mathrm{SINR}}$, whitening gain γ, and information loss $\sin^2(\varphi)$ as a function of bandwidth. Channel and signal parameters: $\mathrm{E}_\mathrm{LOS}/N_0 = 30$ dB, $K_\mathrm{LOS} = 0$ dB, RMS delay spread 17.3 ns; DM: double-exponential PDP, $\gamma_\mathrm{rise} = 5$ ns, $\gamma_\mathrm{dec} = 20$ ns, $\chi = 0.98$; signal: root-raised-cosine pulse, roll-off $R = 0.6$. (See [4] for a detailed description of the model parameters.)

where $\beta^2 = \|\dot{\mathbf{s}}_\tau\|^2/(4\pi^2\|\mathbf{s}_\tau\|^2) = \int_f f^2|S(f)|^2\mathrm{d}f$ is the mean-square bandwidth of the (energy-normalized) transmit pulse $s(t) \overset{\mathcal{F}}{\longleftrightarrow} S(f)$, and $\mathrm{SNR} = |\alpha|^2\|\mathbf{s}_\tau\|^2T_\mathrm{s}/N_0$ is the SNR. (Note that here the norms are without weighting.)

We can decompose the first part of (6) as in (7) to obtain

$$\mathcal{I}_\tau^{(\mathrm{I})} = 8\pi^2\beta_\mathrm{w}^2\mathrm{SINR}\sin^2(\varphi) \tag{8}$$

with the *extended* (mean-square) bandwidth of the whitened pulse $\beta_\mathrm{w}^2 = \|\dot{\mathbf{s}}_\tau\|_\mathcal{H}^2/(4\pi^2\|\mathbf{s}_\tau\|_\mathcal{H}^2)$, the signal-to-interference-and-noise ratio (SINR)

$$\mathrm{SINR} = \frac{|\alpha|^2}{N_0}\|\mathbf{s}_\tau\|_\mathcal{H}^2T_\mathrm{s} \tag{9}$$

and the factor $\sin^2(\varphi) \in [0, 1]$. The weighted norm in (9) accounts for the *reduced SNR* due to the interfering DM, hence the term SINR. Fig. 1 illustrates this parameter as a function of the signal BW. At low BW, it converges to the Ricean K-factor of the channel since all DM interferes with the LOS. At high BW, the LOS is resolved from the DM, hence the SINR converges to the SNR. This interpretation implies that the SINR determines the detection probability of the LOS in DM. It also reflects the amplitude fading of the LOS in DM.

Fig. 1 also shows $\sin^2(\varphi)$ which quantifies the information-loss due to the estimation of the nuisance parameter α (see the appendix). Remember that φ is the angle between $\mathbf{s}_\tau$ and $\dot{\mathbf{s}}_\tau$ in $\mathcal{H}$. Common pulses $s(t)$ (e.g. even or odd waveforms) have derivatives that are orthogonal, i.e. $\sin^2(\varphi) = 1$, hence there is no cost for the estimation of α. However, this property is lost in nonstationary noise when the whitening operation makes the pulse shape asymmetric. The figure shows an information loss at an intermediate range of BW.

Unfortunately the extended bandwidth β_w^2 in (8) is influenced by the whitening, which obscures the signal-bandwidth dependence quantified by the original β^2. For this reason, we introduce the *whitening gain* $\gamma = \beta_\mathrm{w}^2/\beta^2 \geq 1$ that captures the SINR gain due to the whitening and obtain

$$\mathcal{I}_\tau^{(\mathrm{I})} = 8\pi^2\beta^2\gamma\mathrm{SINR}\sin^2(\varphi) \tag{10}$$

$$= 8\pi^2\beta^2\widetilde{\mathrm{SINR}}. \tag{11}$$

In the second line, we introduce the *effective* SINR, $\widetilde{\mathrm{SINR}}$ to arrive at a similarly compact form as in the AWGN case (7). The effective SINR can also be written as

$$\widetilde{\mathrm{SINR}} = \mathrm{SNR}\frac{\|\dot{\mathbf{s}}_\tau\|_{\mathcal{H}}^2}{\|\dot{\mathbf{s}}_\tau\|^2}\sin^2(\varphi) \tag{12}$$

which highlights that it quantifies a *loss of SNR* due to (i) the influence of whitening on the pulse derivative $\dot{\mathbf{s}}_\tau$ and (ii) the impact of estimating the nuisance parameter α.

As seen from Fig. 1, the $\widetilde{\mathrm{SINR}}$ follows the SINR at high BW but it reverses its trend at low BW and converges again towards the SNR due to the impact of γ. This reflects the pulse distortion of the LOS due to DM: The pulse distortion is negligible at very high BW because there is hardly any DM to interfere with the LOS due to the high time resolution (the UWB case). It is also negligible at very low BW, where *all* DM interferes with the LOS and we obtain the flat-fading case.

With the illustration of Fig. 1, the following *bandwidth scaling* can be observed from (11): Due to β^2, the REB would decrease reciprocally with the signal BW. This behavior is well-known from the AWGN case (7). However, the $\widetilde{\mathrm{SINR}}$ also scales with the BW. This yields, for large BWs (> 10 MHz in Fig. 1), a super-linear scaling of the REB with the bandwidth-inverse since increasing the BW reduces the interfering DM. Surprisingly, this effect is reversed at very low BWs where the flat-fading case is approached.

IV. Position Error Bound and Diversity Gain

The PEB is the CRLB on the position estimation error,

$$\sqrt{\mathbb{E}\left\{\|\mathbf{p}-\hat{\mathbf{p}}\|^2\right\}} \geq \mathcal{P}\{\mathbf{p}\} = \sqrt{\mathrm{tr}\left\{\boldsymbol{\mathcal{I}}_{\mathbf{p}}^{-1}\right\}}, \tag{13}$$

the inverse of the so-called *equivalent* Fisher information matrix (EFIM) $\boldsymbol{\mathcal{I}}_{\mathbf{p}}$ on the agent position $\mathbf{p}$ [1]. The block inversion lemma and a matrix transformation are used to obtain the EFIM from the FIM on the signal parameters $\boldsymbol{\psi}_\ell$ [1], [4], where we reintroduce multiple measurements $\ell = 1, 2, \ldots, L$. Assuming independence of these range measurements, the EFIM $\boldsymbol{\mathcal{I}}_{\mathbf{p}}$ can be written as [1], [4]

$$\boldsymbol{\mathcal{I}}_{\mathbf{p}} = \frac{8\pi^2\beta^2}{c^2}\sum_{\ell=1}^{L}\widetilde{\mathrm{SINR}}_\ell \mathbf{D}_{\mathrm{r}}(\boldsymbol{\phi}_\ell) \tag{14}$$

where $\mathbf{D}_{\mathrm{r}}(\boldsymbol{\phi}_\ell)$ is the ranging direction matrix (cf. [1]) for measurement ℓ, a rank-one matrix with an eigenvector in the direction in which the obtained ranging information points. This direction is related to the geometry of the involved agent and anchors, expressed by $\boldsymbol{\phi}_\ell$. For active radiopositioning, it simply points in the angle-of-arrival (AoA) of the LOS component, the direction of vector $(\mathbf{p}-\mathbf{a}_\ell)$. See [1], [2], [4] for the definition of $\mathbf{D}_{\mathrm{r}}(\boldsymbol{\phi}_\ell)$ in other scenarios. The derivation of (14) assumes that the nuisance parameters α_ℓ are estimated independently, i.e. no phase coherence is required between individual measurements.

We review from [1] the valuable insight gained from (14), adopting the REB from Section III: In particular, each measurement adds a positive term to the EFIM in direction of the eigenvector of $\mathbf{D}_{\mathrm{r}}(\boldsymbol{\phi}_\ell)$ and hence reduces the PEB in this direction; the $\widetilde{\mathrm{SINR}}_\ell$ determines the magnitude of this contribution (cf. ranging intensity information (RII) in [1]); the effective bandwidth β scales the EFIM. Any increase corresponds to a decreased PEB.

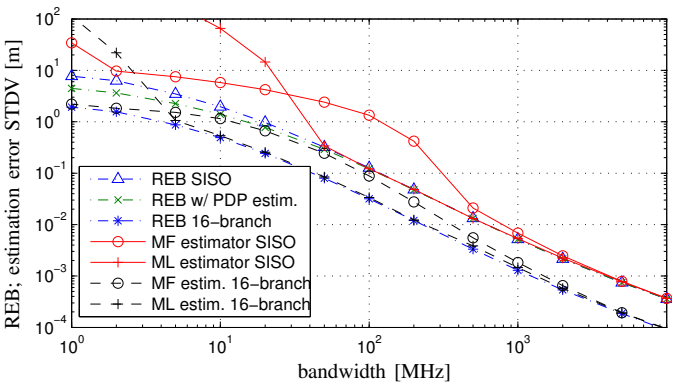

Fig. 2. Ranging error bound and simulated range estimation standard deviations. Channel and signal parameters are as in Fig. 1; number of channel realizations for simulation $N_{\mathrm{sim}} = 1000$.

We can also use (14) to evaluate the impact of diversity. Assume that multiple measurements are conducted with an array of closely-spaced antennas. The ranging directions $\mathbf{D}_{\mathrm{r}}(\boldsymbol{\phi}_\ell)$ of those measurements are equal, therefore the *diversity gain* corresponds to the sum of their $\widetilde{\mathrm{SINR}}$-values. Mathematically, we group the measurements into N sets $\mathcal{N}_n$ having equivalent ranging directions $\mathbf{D}_{\mathrm{r}}(\boldsymbol{\phi}_n)$ and rewrite (14) as

$$\boldsymbol{\mathcal{I}}_{\mathbf{p}} = \frac{8\pi^2\beta^2}{c^2}\sum_{n=1}^{N}\left[\sum_{\ell\in\mathcal{N}_n}\widetilde{\mathrm{SINR}}_\ell\right]\mathbf{D}_{\mathrm{r}}(\boldsymbol{\phi}_n). \tag{15}$$

The Fisher information hence scales linearly with the number of combined measurements (if all measurements have the same $\widetilde{\mathrm{SINR}}$). And there is a second benefit resulting from diversity combining: the detectability of the LOS in noise will be enhanced too, just as the bit (detection) error rate is improved by diversity combining in communications.

It is interesting to compare this result to a ranging system with antenna-array *beamforming*. Assume that the beam is ideally steered towards the AoA by *coherently* combining M branch measurements. Such coherent processing increases the LOS amplitude by the same factor M as the variances of the DM and of the AWGN. The SINR is hence increased M-fold, while the INR is unchanged, implying that the effective $\widetilde{\mathrm{SINR}}$ sees exactly the same M-fold increase as in (15). This result is rather surprising since (15) is based on independent range measurements in contrast to the coherent processing. The advantage of the beamforming approach lies in the possibility to also resolve AoA information, cf. [10]. Furthermore, a uniform angle power spectrum is assumed for the DM to get this M-fold scaling of the interference power. Other angle spectra will change the SINR-gain obtained with beamforming.

V. Performance Results

The REB is illustrated in Fig. 2 and compared to the standard deviation (STDV) of the estimation error for two estimators. Circles mark the performance of a "naïve" matched

filter (MF) estimator that simply convolves the received signal by the transmit pulse and searches for the highest peak. At BWs less than 500 MHz, the performance of this estimator clearly deviates from the theoretical bound. This is due to a positive bias and estimation outliers induced by the DM.

Here, proper consideration of the pulse distortion can be highly beneficial, as seen from the simulation result for a maximum-likelihood (ML) estimator (marked by '+') which performs a whitening operation prior to the estimation of the ToA (considering DM plus AWGN as noise processes). In the single-input, single-output (SISO) case, this estimator achieves the REB down to a BW in the order of 50 MHz (at the simulated channel and signal parameters, which are considered to reflect a realistic indoor environment, cf. [4], [9]). The potential performance gain reaches a factor of ten in this region and an STDV in the order of 30 cm.

At even lower BW, the ML estimator fails and the MF estimator suddenly becomes more robust. Failure of the ML estimator is due to the high risk of outliers: The SINR-value quantifies the SNR after the whitening operation and hence determines the detectability of the LOS signal in the resulting noise floor. The ML estimator fails because the SINR drops well below 10 dB for a BW less equal 20 MHz (cf. Fig. 1). Here the MF estimator can increasingly *make use* of DM in the sense that it exploits the signal power contained in the diffuse part in addition to the signal power in the LOS component. In the limiting case, flat fading and AWGN are the remaining impairments, hence the ranging performance will be bounded by the instantaneous SNR and the BW β^2 as in (7). However, the performance is at a very poor level due to the low BW.

Fig. 2 also shows the improvement obtained from antenna diversity. The REB as well as the STDV of the MF and ML estimators are shown for a 16-branch case, corresponding e.g. to a 4×4 antenna configuration. The figure illustrates the expected factor-of-four improvement of the STDV and also the reduced outlier probability. The ML estimator achieves now an STDV better than 10 cm at 50 MHz and it still operates at the bound at 10 MHz with an error STDV of about 0.5 m.

VI. Conclusions

The ranging and position error bounds have been analyzed for LOS signals in dense multipath (DM), evaluating the impact of signal bandwidth and diversity. DM is an interference to the LOS signal, which causes amplitude fading and signal distortions. Both effects have been quantified using a Gaussian model for the DM. Diversity combining can compensate a performance loss at reduced bandwidth and enhance the detectability of the LOS in presence of DM. The Fisher information scales faster than quadratically with bandwidth but only linearly in the number of independent measurements.

Appendix

This appendix derives the equivalent Fisher information (EFI) (6) for the delay parameter τ. The Fisher information matrix (FIM) for parameter vector $\boldsymbol{\psi}$ is [12]

$$\boldsymbol{\mathcal{I}}_{\boldsymbol{\psi}} = \mathbb{E}_{\mathbf{r}|\boldsymbol{\psi}} \left\{ \left[\frac{\partial}{\partial \boldsymbol{\psi}} \ln f(\mathbf{r}|\boldsymbol{\psi}) \right] \left[\frac{\partial}{\partial \boldsymbol{\psi}} \ln f(\mathbf{r}|\boldsymbol{\psi}) \right]^{\mathrm{T}} \right\} \quad (16)$$

leading, for the Gaussian likelihood (3), to (cf. [12, Sec. 15.7])

$$[\boldsymbol{\mathcal{I}}_{\boldsymbol{\psi}}]_{1,1} = 2|\alpha|^2 \dot{\mathbf{s}}_\tau^{\mathrm{H}} \mathbf{C}_{\mathrm{n}}^{-1} \dot{\mathbf{s}}_\tau + \mathrm{tr}\left[\mathbf{C}_{\mathrm{n}}^{-1} \frac{\partial \mathbf{C}_{\mathrm{n}}}{\partial \tau} \mathbf{C}_{\mathrm{n}}^{-1} \frac{\partial \mathbf{C}_{\mathrm{n}}}{\partial \tau} \right] \quad (17)$$

$$[\boldsymbol{\mathcal{I}}_{\boldsymbol{\psi}}]_{1,2} = [\boldsymbol{\mathcal{I}}_{\boldsymbol{\psi}}]_{2,1} = 2\Re\{\alpha\} \mathbf{s}_\tau^{\mathrm{H}} \mathbf{C}_{\mathrm{n}}^{-1} \dot{\mathbf{s}}_\tau \quad (18)$$

$$[\boldsymbol{\mathcal{I}}_{\boldsymbol{\psi}}]_{1,3} = [\boldsymbol{\mathcal{I}}_{\boldsymbol{\psi}}]_{3,1} = 2\Im\{\alpha\} \mathbf{s}_\tau^{\mathrm{H}} \mathbf{C}_{\mathrm{n}}^{-1} \dot{\mathbf{s}}_\tau \quad (19)$$

$$[\boldsymbol{\mathcal{I}}_{\boldsymbol{\psi}}]_{2,2} = [\boldsymbol{\mathcal{I}}_{\boldsymbol{\psi}}]_{3,3} = 2\mathbf{s}_\tau^{\mathrm{H}} \mathbf{C}_{\mathrm{n}}^{-1} \mathbf{s}_\tau \quad (20)$$

$$[\boldsymbol{\mathcal{I}}_{\boldsymbol{\psi}}]_{2,3} = [\boldsymbol{\mathcal{I}}_{\boldsymbol{\psi}}]_{3,2} = 0 \quad (21)$$

where $\dot{\mathbf{s}}_\tau = \partial \mathbf{s}_\tau / \partial \tau$ is the derivative of the pulse $s(t-\tau)$.

The covariance matrix of DM is $\mathbf{C}_{\mathrm{c}} = \bar{\mathbf{S}}^{\mathrm{H}} \mathbf{S}_\nu \bar{\mathbf{S}}$, where $\bar{\mathbf{S}} = [\mathbf{s}_0, \cdots, \mathbf{s}_{N-1}]^{\mathrm{T}} \in \mathbb{R}^{N \times N}$ is a signal matrix with $\mathbf{s}_i = [s((-i)T_{\mathrm{s}}), \ldots, s((N-1-i)T_{\mathrm{s}})]^{\mathrm{T}}$ and $\mathbf{S}_\nu$ is a diagonal matrix containing the PDP, i.e. $[\mathbf{C}_{\mathrm{c}}]_{n,m} = \sum_{i=0}^{N-1} T_{\mathrm{s}} S_\nu(iT_{\mathrm{s}}) s((n-i)T_{\mathrm{s}}) s((m-i)T_{\mathrm{s}})$. We decompose $\mathbf{C}_{\mathrm{c}} = \mathbf{U}\boldsymbol{\Lambda}\mathbf{U}^{\mathrm{H}}$ where the columns of $\mathbf{U}$ are an orthonormal basis for a Karhunen-Loève expansion of the noise process. The entries of the diagonal matrix $\boldsymbol{\Lambda}$ thus quantify the DM power in these coordinates. This yields $\mathbf{C}_{\mathrm{n}}^{-1} = \mathbf{U}(\boldsymbol{\Lambda} + \sigma_{\mathrm{n}}^2 \mathbf{I}_N)^{-1} \mathbf{U}^{\mathrm{H}}$.

The EFI for the delay τ corresponds to the Schur complement of the (1,1)-element (17) (cf. [1]). Using (4), we obtain

$$\mathcal{I}_\tau = 2\frac{|\alpha|^2}{\sigma_{\mathrm{n}}^2} \|\dot{\mathbf{s}}_\tau\|_{\mathcal{H}}^2 \left(1 - \frac{|\langle \dot{\mathbf{s}}_\tau, \mathbf{s}_\tau \rangle_{\mathcal{H}}|^2}{\|\dot{\mathbf{s}}_\tau\|_{\mathcal{H}}^2 \|\mathbf{s}_\tau\|_{\mathcal{H}}^2} \right) + \mathrm{tr}\,[\bullet] \quad (22)$$

where $\mathrm{tr}\,[\bullet]$ is a placeholder for the second part of (17). The subtractive term illustrates the information loss due to the estimation of α. It arises from the terms (18)–(21). We introduce the factor $\sin^2(\varphi)$ for this expression, where φ is the angle between $\dot{\mathbf{s}}_\tau$ and $\mathbf{s}_\tau$ in $\mathcal{H}$, and obtain (6).

References

[1] Y. Shen and M. Win, "Fundamental limits of wideband localization; Part I: A general framework," *IEEE Trans. Inf. Theory*, vol. 56, no. 10, pp. 4956–4980, Oct. 2010.

[2] H. Godrich, A. Haimovich, and R. Blum, "Target Localization Accuracy Gain in MIMO Radar-Based Systems," *IEEE Trans. Inf. Theory*, vol. 56, no. 6, pp. 2783 –2803, June 2010.

[3] D. Dardari, A. Conti, U. Ferner, A. Giorgetti, and M. Win, "Ranging with ultrawide bandwidth signals in multipath environments," *Proc. IEEE*, vol. 97, no. 2, pp. 404–426, Feb. 2009.

[4] E. Leitinger, P. Meissner, C. Ruedisser, G. Dumphart, and K. Witrisal, "Evaluation of position-related information in multipath components for indoor positioning," *IEEE J. Sel. Areas Commun.*, vol. 33, no. 11, pp. 2313 – 2328, Nov. 2015.

[5] A. Richter and R. Thoma, "Joint maximum likelihood estimation of specular paths and distributed diffuse scattering," in *IEEE Vehicular Technology Conference, VTC 2005-Spring*, 2005.

[6] S. Bartoletti, W. Dai, A. Conti, and M. Z. Win, "A mathematical model for wideband ranging," *IEEE Journal of Selected Topics in Signal Processing*, vol. 9, no. 2, pp. 216–228, March 2015.

[7] M. Z. Win, A. Conti, S. Mazuelas, Y. Shen, W. M. Gifford, D. Dardari, and M. Chiani, "Network localization and navigation via cooperation," *IEEE Communications Magazine*, vol. 49, no. 5, pp. 56–62, May 2011.

[8] W. Dai, Y. Shen, and M. Z. Win, "Distributed power allocation for cooperative wireless network localization," *IEEE J. Sel. Areas Commun.*, vol. 33, no. 1, pp. 28–40, Jan 2015.

[9] S. Hinteregger, E. Leitinger, P. Meissner, J. Kulmer, and K. Witrisal, "Bandwidth dependence of the ranging error variance in dense multipath," in *Proc. Europ. Signal Proc. Conf. (EUSIPCO)*, 2016, submitted.

[10] Y. Han, Y. Shen, X. Zhang, M. Win, and H. Meng, "Performance limits and geometric properties of array localization," *IEEE Trans. Inf. Theory*, vol. 62, no. 2, pp. 1054–1075, Feb 2016.

[11] S. Hinteregger, E. Leitinger, P. Meissner, and K. Witrisal, "MIMO gain and bandwidth scaling for RFID positioning in dense multipath channels," in *IEEE Intern. Conf. on RFID*, Orlando, FL, May 2016.

[12] S. Kay, *Fundamentals of Statistical Signal Processing: Estimation Theory*. Prentice Hall Signal Processing Series, 1993.